Modeling of RF thermal ablation taking into account the temperature dependence of the tissue properties

Douglas. Deás Yero, Fidel Gilart González, Dirk Van Troyen and Guy A. E. Vandenbosch

ABSTRACT / *RESUMEN*

The outcome of radio frequency thermal ablation (RFTA) is significantly affected by the tissue electrical conductivity; thus, understanding the changes of this property during heating is fundamental to suitably model the medical procedure. In this work a reasonable procedure is proposed for selecting the appropriate experimental data of the temperature dependence of electrical conductivity for the simulation taking into account the heating rate at which the data was acquired and the power that will be delivered to the electrodes in the RFTA situation of interest, based on the computing of the time average of the heating rate in a representative point of the ablation zone. The numerical results confirmed that the use of lower frequencies (20 kHz) than currently used during RFTA (450 kHz) may result in preferential heating of the tumor and consequently in less damage on healthy tissue. Also, the effect on the computed thermal lesion size of three different models of the temperature dependence of electrical conductivity used for the simulation of a RFTA situation at 20 and 450 kHz, entailing the presence of three materials with different dielectric properties (normal liver tissue, tumor gel phantom and muscle saline phantom) was investigated. The results demonstrated that not only the initial (baseline) electrical conductivity is important in predicting the lesion size, but also it is the model of the temperature dependence of electrical conductivity.

Key words: Radio frequency thermal ablation (RFTA), 2D FEM modeling, electro-thermal properties of tissues.

El resultado de la terapia de ablación térmica por radiofrecuencia (RFTA) es significativamente afectado por la conductividad eléctrica del tejido; por eso la comprensión de los cambios de esta propiedad durante el calentamiento es fundamental para modelar adecuadamente el procedimiento médico. En este trabajo se propone un procedimiento razonable para seleccionar los datos experimentales apropiados de la dependencia de la conductividad eléctrica con la temperatura para la simulación teniendo en cuenta el ritmo de calentamiento a la que fueron adquiridos los datos y la potencia a suministrar a los electrodos en la situación de RFTA de interés, basado en la computación del promedio temporal de la velocidad de calentamiento en un punto representativo de la zona de ablación. Los resultados numéricos confirmaron que la utilización de frecuencias más bajas (20 kHz) que las actualmente en uso durante la RFTA (450 kHz) puede producir un calentamiento preferencial del tumor y por consiguiente menos daño en el tejido sano. También se investigó el efecto sobre el tamaño computado de la lesión térmica, de tres modelos diferentes de la dependencia de la conductividad eléctrica con la temperatura, usados para la simulación de una situación de RFTA a 20 y 450 kHz que acarrea la presencia de tres materiales con propiedades dieléctricas diferentes (tejido hepático normal, phantom gel del tumor y phantom salino del tejido muscular). Los resultados demostraron que no sólo la conductividad eléctrica inicial (la línea base) es importante para predecir el tamaño de la lesión, sino también el modelo de la dependencia de la conductividad eléctrica con la temperatura.

Palabras claves: ablación térmica por radiofrecuencia (RFTA), modelado FEM 2D, propiedades electro térmicas de los tejidos.

Modelación de la ablación térmica por RF teniendo en cuenta la dependencia de las propiedades del tejido con la temperatura.

Douglas Deás Yero, Fidel Gilart González, Dirk Van Troyen, Guy A.E. Vandenbosh

1. - INTRODUCTION

The use of the electromagnetic energy for heating in health services and clinical applications has been expanded in the last decades. Some examples include planning and monitoring thermal treatments facilitating radiofrequency (RF), microwave (MW), focused ultrasound (FUS), and laser energy, where the goal is to obtain defined temperatures in a targeted tissue region [1]. Specifically, the RF thermal ablation (RFTA) is currently the most widely used ablative technique for the treatment of a localized tumor lesion, resulting in a minimally invasive surgery, less pain, lesser damage to normal tissue and lesser recovery period over all the classical methods [2].

The overall survival rate of the RFTA is comparable with the open surgery when it is used to treat early and small tumors. Several recent studies also show that RFTA can induce an immune response in tumors that are remote to the tumor being ablated. The characteristic of immunotherapy makes RFTA have a promising future with regard to expanding its application for different phases of tumors in different locations. However, the most critical factor that hinders RFTA from developing or improving is its failure in the treatment of large tumors (i.e. ≥ 3 cm in diameter) [3].

Several studies highlight the importance of electrical conductivity on the outcome of RFTA using numerical simulations [1, 4-7]; however, most focus only on numerical simulations without integrating data from conductivity measurements or from RF ablation experiments. The electrical conductivity and permittivity of various tissues have been measured at body temperature for several decades [8-12], but their variation during the coagulation process was only studied in recent years. Ryan et al [13] measured electrical conductivity of brain, muscle, liver and fat tissue at 500 kHz between 40 and 90 °C, revealing an increase of conductivity with temperature, and irreversible changes above 60 °C. Pop et al [3] studied the changes in the dielectric properties of ex vivo kidney and fat tissue at 460 kHz, during heating. A reversible temperature-dependent effect and an irreversible effect due to structural changes were found. Zurbuchen et al [14] measured ex vivo and in vivo the temperature dependence of the electrical conductivity of porcine liver tissue at 470 kHz. These measurements, however, were performed either at constant temperature or in quasi-static conditions with slow heating in a water bath. Recently, Macchi et al [7] measured ex vivo the electrical conductivity and permittivity of porcine liver tissue at 480 kHz during uniform heating up to 100 ℃ at constant slow and fast heating rates, revealing that the conductivity increased with increasing temperature, but above 60 °C different trends were observed for high and low heating rate experiments. More recently, Deás et al [15] measured ex vivo the electrical conductivity and permittivity of porcine liver tissue at RF frequencies from 5 kHz to 500 kHz during uniform heating up to 100 ℃ at constant very slow, slow and fast heating rates, confirming the results of Macchi et al [7].

Devices used clinically for RF tumor ablation all operate in the frequency range of 375–500 kHz due to their development out of electrosurgical units. Haemmerich & Schutt [16] examined whether ablation via electric current at lower RFs provides benefits in terms of targeted tumor heating, as suggested by other prior studies. The potential benefit of lower frequencies than currently used stems from the frequency dependence of electrical tissue conductivity, and particularly the variation of this frequency dependence between normal and cancer tissue. These authors placed normal porcine liver tissue in contact with agar gel having similar conductivity as tumor within 20-450 kHz. They placed a needle electrode with half of the electrically active tip in each layer and performed ablation with electric current applied for 12 min at 30 W, either at 20 or 450 kHz, while measuring temperature via thermocouples 4 and 8 mm from the electrode. Mathematical heat-transfer models were created of an equivalent configuration and temperature profile determined at both frequencies. Computer models using a linear relationship for the temperature dependence of electrical conductivity of the normal liver tissue confirmed the results of the temperature measurements, and showed the ablation zone diameter to be larger within the tumor phantom at 20 kHz compared to 450 kHz. They concluded that heating at low RFs may thus allow targeted heating of tumor tissue and reduced heating of normal tissue.

Recently, a sensitivity analysis was performed by Hall et al [17] on a mathematical model of RFTA in the liver tissue with the purpose of identifying the most important parameters in the model, defined as those that produce the largest changes in the prediction of the lesion size. A simplified RFTA situation was considered, entailing the presence of only one material (the normal liver tissue), and a linear relationship for the temperature dependence of electrical conductivity was used. It was found that the most important parameters in predicting the lesion size were the blood perfusion, the initial (baseline) electrical conductivity and the cell death model.

A little before, Macchi el al [7] investigated the effects of different electrical conductivity models (fast and slow heating interpolating curves, Arrhenius based conductivity fit of the experimental data, slow heating experimental data from Zurbuchen et al [14], and constant $\sigma = \sigma_{37}$) using a simulation framework previously calibrated with experimental RFTA results. As in [17] a simplified RFTA situation was considered, entailing the presence of only one material (the normal liver tissue). The performed simulations showed that all tested models were suitable for the simulation of RFTA as long as the conductivity variation with temperature is taken into account. However, taking into account that in situations typical of in

vivo RFTA, which entail the presence of multiple materials with different dielectric properties (e.g. inclusion of normal and tumor tissue and saline-enhanced RFTA), the effects of different conductivity models may be stronger, the authors of [7] recommended that the conductivity models must also be tested in such more complex situations and that future computational studies should address this topic. A good candidate for conducting such testing is the RFTA situation considered by Haemmerich & Schutt in [16], involving the presence of three materials with different dielectric properties (normal liver tissue, tumor gel phantom and muscle saline phantom). An additional problem to solve is how to select the appropriate experimental data for the simulation, taking into account the heating rate at which the data was acquired and the power that will be delivered to the electrodes in the RFTA considered situation. The solution of these problems is addressed in this work. The new contribution to the RFTA situation considered by Haemmerich & Schutt in [16] is the proposition of a more realistic conductivity model of the liver tissue for the simulation of the ablation process.

2. - MATERIAL AND METHODS

The following sections present a brief description of the computational modeling, mathematical function and the material properties used during simulation of RFTA.

2.1. - COMPUTATIONAL MODELING OF RFTA

The computational modeling of RFTA generally requires the use of numerical methods. The most commonly used techniques include the Finite Element Method (FEM), the Finite Difference Time Domain Method (FDTD), the Method of Moments (MoM) and Radial Basis Collocation Method (RBCM). The Finite Element Method has been used extensively due to its availability in commercial software such as COMSOL Multiphysics and ANSYS, which are capable of coupling electromagnetic field solutions to other physics models such as heat transfer and diffusion [18].

Several researchers have developed for the RF heating one-dimensional models, two-dimensional (2D) models (based on axial symmetry) and three-dimensional (3D) models validated by means of experimental measurements using in vivo, in vitro or phantom of tissue-equivalent material [19]. In 1995, the first 3D RF cardiac ablation model [20] was presented by the most prolific group in theoretical modeling of RF ablation directed by Prof. John G. Webster (University of Wisconsin-Madison). However, for axial symmetric geometries 2D models may be preferable and required to reduce the computational simulation process. Several works have been validated with experimental data with a good agreement during RFTA using axisymmetric geometry 2D modeling [1, 21-25].

Berjano [19] explained the methodology with the main steps in the building and use of a theoretical model in studies on RF heating, including the experimental validation. These steps are basically: 1) observation and simplification of the physical situation, 2) arrangement of the mathematical equations which rule the electrical and thermal phenomena, 3) determination of the boundary conditions, both electrical and thermal, 4) obtaining the physical characteristics (electrical and thermal) of the biological tissues and other materials included in the model, 5) choosing a numerical method in order to computationally or analytically achieve a solution, and 6) conducting the post-processing of the computed results.

We used COMSOL Multiphysics software 5.2a (COMSOL, Zoetermeer, Nederland) to generate the geometric models, assign material properties, assign boundary conditions, generate mesh, and perform the coupled electro-thermal analysis. A coupled analysis is required since electrical properties change with temperature, and therefore, the electric field problem has to be accordingly modified at each time step. The whole analysis was performed on a PC equipped with a Core i3 2.6 GHz CPU and 8 GB of RAM memory. Figure 1 shows the complete work flow chart during the simulation based on [22].
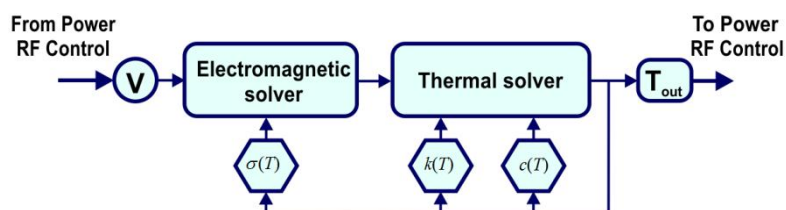

Figure 1

Flow chart representation of the simulation setup.

2.2. - THERMO-ELECTRICAL FEM FORMULATION

The modeling of RF heating is based on a time domain analysis of a coupled electro-thermal problem where the temperature rise in the tissues is usually obtained by solving the Bio-heat equation [23-25]:

$$\rho c \frac{\partial T}{\partial t} = \vec{\nabla} \cdot k(T)\vec{\nabla}T + q - Q_p + Q_m \tag{1}$$

where, for a specific material or tissue, ρ is the volumetric mass density (kg/m^3), c is the specific heat capacity (J/kg·K), $k(T)$ is the thermal conductivity (W/m·K) and $T = T(r, t)$ is the temperature (K). Q_p represent the heat loss through blood perfusion (W/m^3), this term is negligible in some cases of RF heating, such as non vascular tissues, however is always considered in cases of tissues with a high degree of perfusion, such as liver [19]. This term is mathematically expressed as:

$$Q_p = \rho_b \omega_b(T) c_b (T - T_b) \tag{2}$$

where ρ_b is the blood volumetric mass density (kg/m^3), $\omega_b(T)$ is the blood perfusion velocity (s^{-1}), c_b is the specific heat capacity of blood (J/kg·K) and T_b is the blood temperature (assumed to be 37 °C). On the other hand, Q_m is the metabolic heat generation (W/m^3) but usually ignored due to its minimal impact compared to the other heat terms.

The remaining term in equation (1) is the heat source caused by the RF electromagnetic field into the tissue ($q = \vec{J} \cdot \vec{E}$), where $\vec{J}$ and $\vec{E}$ are the electric current density (A/m^2) and the electric field strength (V/m) in the tissue, respectively. A simplified version of Maxwell's equation, known as quasi-static approach, is used to compute the resistive heating during RFTA, since in the frequency range of this technique the wavelength of electric field is several orders of magnitude larger than the size of the active electrode. In this case the electric field strength can be expressed as the gradient of the scalar electric potential, $\vec{E} = -\vec{\nabla}\varphi$, the electric current density is related to the electric field strength by Ohm's law, $\vec{J} = \sigma\vec{E}$, and it is divergence-free. Thus, the electric potential φ(V) satisfies

$$\vec{\nabla} \cdot \sigma(T)\vec{\nabla}\varphi = 0 \tag{3}$$

and the heat source caused by external RF power can be expressed as

$$q = \sigma(T)\left|\vec{\nabla}\varphi\right|^2 \tag{4}$$

Under the influence of an alternating electric field, the electrical conductivity σ(S/m) is actually an effective conductivity ($\sigma = \sigma_s + \sigma_a$), composed of a static term, σ_s, due to the ability of free charges to migrate under the influence of an electric field, and an alternating part, σ_a, caused by the rotation of dipoles as they attempt to align with an alternating applied electric field. The static conductivity contributes to the conductive or resistive losses (Joule losses) of a material, while the alternating conductivity contributes to dielectric losses. The ratio of resistive to dielectric losses depends on the material and the frequency of the applied electric field. For most biological tissues, resistive losses dominate up to several MHz after which dielectric effects begin to contribute. Only at microwave frequencies ($f > 300$ MHz), dielectric losses play a more significant role in the generation of heat. In practice it is only possible to measure the total conductivity σ.

From equation (3) and (4), it is evident that the electrical conductivity strongly affects the distribution of electric potential and Joule losses.

2.3. - MODEL GEOMETRY AND BOUNDARY CONDITIONS

We used the FEM to solve the coupled thermoelectric equations for a cooled needle electrode in a two-layer setup of normal liver tissue and tumor gel phantom, simulating ablations at both 20 and 500 kHz for 12 min at 30 W of power, similar to computational model developed by Haemmerich & Schutt [16]. As in [16] an axial symmetry was assumed for the geometry and thus a 2D axisymmetric analysis was conducted. The geometry and the dimensions of the developed theoretical model are shown in Figure 2. The model consisted of four different domains: air, tumor phantom, liver tissue, and muscle saline phantom. The electrodes were modeled as electric potential boundary conditions.

The cooled needle electrode with an active length of 30 mm was placed in a two-layered (top-half tumor, bottom-half normal tissue) cylinder 90 mm high, and 250 mm in diameter, such that half of the active length was in each layer. An adaptive mesh of 7504 triangular elements was generated in COMSOL Multiphysics with a maximum element size of 1.0 mm in the tumor and liver domains and of 9.25 mm in the rest. Initial convergence tests were performed to confirm that the mesh size was sufficiently small, with a tissue temperature variation of less than 0.1 °C as the convergence criterion. The time was varied between 0 and 720 s with a step of 1 s. A boundary condition of 0 V was applied to the electric potential of

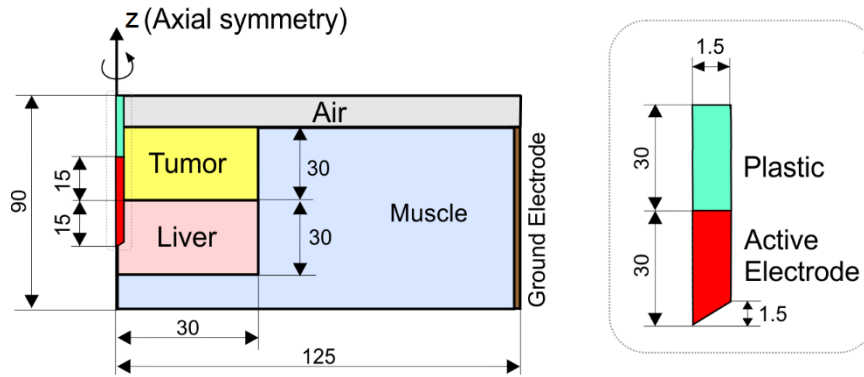outer model boundary representing the ground electrode.

Figure 2

Axisymmetric geometry of the two-dimensional theoretical model (out of scale and dimensions in mm).

As in [16], the initial tissue temperature was set to room temperature (20 °C) in all domains of the problem, and power developed in the simulations of this work was kept at a constant value of 30 W throughout simulation time. In order to keep developed power constant, though tissue properties are changing with increasing temperature, the potential of the electrode was adapted continuously to the current conditions. This was done by setting up an ordinary differential equation which connects the developed power (P) to electrode potential and defining (P) as an integration coupled variable which was updated in every time-iteration. An initial guess of 60 V was taken for the electrode potential. In contrast, for keeping power at a constant value throughout simulation time Fang et al [26] selected a variable power source determined by a proportional–integrative–derivative controller (KP= 32, KI = 1, and KD = 0.001) at constant applied voltage of 30 V. Another type of temperature-controlled RFA in FEM modeling can be used to avoid tissue carbonization [27].

Similar to [16], the internal cooling of the needle electrode via circulating cooled water was simulated by applying a constant temperature boundary of 10 °C to the needle surface (note that a prior study showed that the tissue temperature profile is not sensitive to changes in cooling temperature) [28]. On the external boundaries of the thermal problem an open boundary condition was used.

2.4. - TEMPERATURE DEPENDENCE OF ELECTRICAL CONDUCTIVITY

At the present time many numerical studies assume that the temperature-dependent behavior of the electrical conductivity of liver tissue up to a temperature of 100 ºC is similar to that of an equivalent sodium chloride solution [21]. Many of these use linear expressions for this dependence similar to that derived by Stogryn [29] for a given temperature (T) and normality (N). Other authors such as Haemmerich & Schutt [16] use these linear dependences in the form:

$$\sigma(T) = \sigma_0[1 + k_\sigma(T - T_0)] \tag{5}$$

where σ_0 is the electrical conductivity (S/m) at the reference temperature T_0 of the tissue at a specific frequency, k_σ is the temperature coefficient usually selected between (0.006 – 0.02) °C^{-1} for liver tissue. In [16] T_0 was set equal to 20 ºC, and k_σ equal to 0.0162 °C^{-1}. Similar to [16], we modeled the electrical conductivities of tumor gel phantom and of muscle saline phantom as a 0.12% and 0.25% NaCl solution, respectively.

When considering temperatures of up to 100 ºC and above, the electrical conductivity of the liver tissue is commonly set to increase linearly with temperatures of up to 100°C and to drop rapidly to an almost zero value as tissue water is converted to gas for temperatures over 100°C. However, there are several discrepancies about the rate and type of this increase and the rate of this drop. Trujillo & Berjano [1] suggested that the temperature dependence of σ below 100 °C can be modeled equally well either by using a linear or exponential increase or an increase rate of between +1.5 %/°C and +2 %/°C. Likewise, once the temperature reaches 100 °C, the change in σ caused by dehydration can be modeled equally well by using an abrupt drop of either two or four orders of magnitude between 100 °C and 105 °C. Hall et al [17] used a piecewise linear continuous function as in equation 6:

$$\sigma(T) = \begin{cases} \sigma_0[1 + k_\sigma(T - T_0)] & T \le T_u \\ [\sigma_{vap} - \sigma_0(1 + k_\sigma(T_u - T_0))](T - T_u)/5 + \sigma_0[1 + k_\sigma(T_u - T_0)] & T_u < T \le T_u + 5 \\ \sigma_{vap} & T_u + 5 < T \end{cases} \quad (6)$$

where σ_{vap} is the conductivity of vaporized tissue, which was assumed to be two to four orders of magnitude smaller than σ_0, and T_u is the upper temperature when the phase change occurs.

Since, to date, there are few experimental measurements on the temperature-dependence of the electrical conductivity of liver tissue, we used an experimental data at two RF frequencies (20 and 500 kHz) obtained in a previous study by Deás et al [15] at three different heating rates and temperatures of up to 100 ℃. For this work the linear equation 5 was used only to compare the simulation results with those obtained using the experimental data of Deás et al [15].

Tissue is a heterogeneous material containing water, dissolved organic molecules, macromolecules, ions, and insoluble matter. The constituents are highly organized in cellular and subcellular structures forming macroscopic elements and soft and hard tissues. The presence of ions plays an important role in the interaction with an electric field, providing means for ionic conduction and polarization effects. Ionic charge drift creates conduction currents and also initiates polarization mechanisms through charge accumulation at structural interfaces, which occur at various organizational levels. As usual, the conductivity model used in this work for modeling and simulating RFTA is a descriptive model, imparting no definite information on the polarization mechanisms; the measured dielectric properties represent the bulk response of the tissue. Assigning effective parameters to a heterogeneous medium is equivalent to treating it as homogeneous where these parameters are concerned; in this case, its structural components are much finer than the wavelength of the field probing it.

2.5. - TEMPERATURE DEPENDENCE OF THERMAL CONDUCTIVITY

There are several criterial about the temperature dependence of thermal conductivity $k(T)$ used during RFTA theoretical models. Trujillo & Berjano [1] studied the different functions used to model the thermal dependence of k as a constant value and as a piecewise continuous function. They found that, the temperature dependence of k can be ignored, and hence a constant value can be used, since the different approaches proposed in previous modeling studies provided similar results. The great discrepancies between these functions are found for temperatures of up to 100 °C. However, the most commonly used approximation for liver tissue considers a linear increase of k at temperatures below 100 °C. Above 100 °C, k has been assumed to be constant as described by the following piecewise continuous function [21]:

$$k(T) = \begin{cases} k_0 + 0.0013\,(T - T_0) & T \le 100\,℃ \\ k(100) & T > 100\,℃ \end{cases} \quad (7)$$

where $k_0 = 0.502$ W/(m. K) at $T_0 = 25$ °C. In contrast, for the same tissue Haemmerich & Schutt [16] used in their study the following variations of k with temperature:

$$k(T) = k_{20} + 0.0008\,T(℃) \quad (8)$$

where $k_{20} = 0.498$ W/(m.K) is the thermal conductivity at 20 °C. The linear dependence (8) was also used in our work.

2.6. - SPECIFIC HEAT CAPACITY

The specific heat capacity of the liver is available for multiple species in a variety of conditions. For normal tissue at physiological temperatures, the mean value is 3700 J/(kg.K) and it is not clear whether the variations seen are due to measurement uncertainty, variations between species, or variations within a species. Therefore, the effects on the model predictions have been studied within the range of the specific heat capacity between (3600 - 4000) J/(kg.K) [17]. Another advantage of choosing this range is that it also includes the specific heat capacity of coagulated tissue. The temperature dependence of the specific heat capacity is often omitted in mathematical models of RFTA [17]. However, Haemmerich et al [30] reported no significant change of specific heat capacity below 65.0 °C and an increased value by about 17% in the range of 65–83.5 °C. For modeling the temperature dependence of the specific heat capacity, we utilized a piecewise function as in equation 9 by Dos Santos et al [31] and Haemmerich & Schutt [16]

$$c(T) = \begin{cases} c_0 & T \le 63.5\,℃ \\ c_0 + k_c(T - 63.5) & T > 63.5\,℃ \end{cases} \quad (9)$$

where c_0 is the initial specific heat capacity in J/(kg.K) and $k_c = 28.9$ J/(kg.K^2).

2.7. - THERMAL DAMAGE

Thermal damage processes in cells and tissues are usually quantified by kinetic models based on a first-order rate process, which are valid assuming that a single biological molecular species (e.g. one type of protein) is responsible for the thermal denaturation. The Arrhenius model [32-33] is a mathematical description based on first order kinetics to predict cell survival after subjecting cells to a particular temperature history, and is commonly used for predicting thermal damage after ablation exposures [34]. To determine the boundaries of cell death, we utilized an Arrhenius damage model, as shown in (10), where thermal damage function $\Omega(t)$ is related to the expected cellular survival fraction, $\theta_s(t)$, as shown in (11)

$$\Omega(t) = \int_0^t A e^{\frac{-E_a}{RT(\tau)}} d\tau \tag{10}$$

$$\theta_s(t) = \frac{c(t)}{c(0)} = e^{-\Omega(t)} \tag{11}$$

where A is the frequency factor (s^{-1}), E_a is the activation energy (J·mol^{-1}), $T(\tau)$ is the absolute temperature (kelvin) as a function of time, $c(t)$ represents the concentration of undamaged cells as a function of time, $c(0)$ is the initial concentration of undamaged cells prior to heating, and R is the universal gas constant (8.314 J/mol·K). Similar to Haemmerich & Schutt [16], we used $A = 2.984 \times 10^{80}$ s^{-1} and $E_a = 5.064 \times 10^5$ J·mol^{-1}. These values were shown in a previous experimental study by Breen et al [35] to accurately predict the cell death boundary in an animal model when used with a threshold value of 4.6 for $\Omega(t)$ (which corresponds to 99.0% cell death). In contrast, for the threshold of tissue death expressed by $\Omega(t) = 1$, which means a 63.21% probability of cell death, recently Fang et al [26] have used the following values for the liver and tumor tissues ($A = 7.390 \times 10^{39}$ s^{-1} and $A = 3.247 \times 10^{43}$ s^{-1}) and ($E_a = 2.577 \times 10^5$ J·mol^{-1} and $E_a = 2.814 \times 10^5$ J·mol^{-1}). From (11) the fraction of death tissue (θ_d) can be expressed as:

$$\theta_d(t) = 1 - e^{-\Omega(t)} \tag{12}$$

Similar to Macchi et al [7], in our analysis the Arrhenius formulation was used also to model the changes in the electrical conductivity of liver tissue caused by irreversible structural changes during heating. As in [7], the resulting equation, used to describe the changes in the electrical conductivity as a result of any thermal history, is as follows:

$$\sigma(T, t) = \sigma_{37}[1 + \alpha(T - 37) + \beta\theta_d(t) - \gamma(T - 37)^8] \tag{13}$$

where T is the temperature (°C), σ_{37} is the electrical conductivity at 37 °C, and α, β and γ are model parameters. The values of the model parameters (A, E_a, α, β and γ) that minimized the root-mean-square error between the experimental data and model output were determined using an unconstrained nonlinear optimization fit algorithm, which finds the minimum of a scalar function of several variables, starting at an initial estimate. For the changes in the electrical conductivity at 450 kHz the following set of parameters was obtained with a root-mean-square error of 1.0438 %: $A = 1.2974 \times 10^{13}$ s^{-1}, $E_a = 1.05 \times 10^5$ J·mol^{-1}, $\alpha = 1.26 \times 10^{-2}$ °C^{-1}, $\beta = 1.25$ and $\gamma = 2.0 \times 10^{-15}$ °C^{-8}. Correspondingly, for the changes in the electrical conductivity at 20 kHz the following parameters were obtained with a root-mean-square error of 1.2843 %: $A = 5.9681 \times 10^{15}$ s^{-1}, $E_a = 1.21 \times 10^5$ J·mol^{-1}, $\alpha = 1.26 \times 10^{-2}$ °C^{-1}, $\beta = 3.77$ and $\gamma = 3.4 \times 10^{-15}$ °C^{-8}.

3. - RESULTS AND DISCUSSION

Attending the recommendations in [7], in this work three different electrical conductivity models (interpolating curve of the appropriate experimental data, linear function of temperature from Haemmerich & Schutt [16], and constant $\sigma = \sigma_{37}$) for normal liver tissue were investigated in an in vitro RFTA situation which entail the presence of three materials with different dielectric properties (normal liver tissue, tumor gel phantom and muscle saline phantom). Although here an Arrhenius-based conductivity model ($\sigma(T, t)$ equation (13)) was also obtained, contrary to [7] we consider that this model is not appropriate for the simulation of RFTA since it adjusts the conductivity based on the local thermal history, whereby this history should be known a priori.

The meaning of "the appropriate experimental data" needs to be explained. Usually, when simulating the RFTA a model of the temperature dependence of electrical conductivity is used, based on experimental data acquired at a constant heating rate in time and space, however in the RFTA typical situations the heating rate varies with time and is not uniform through the tissue. Therefore, the question arises about how to select the appropriate experimental data for the simulation, taking into account the heating rate at which the data was acquired and the power that will be delivered to the electrodes in the RFTA considered situation. The obtaining of the precise solution to this problem is a very complicated issue; however it is possible to obtain a reasonable approximate solution. In this work such a solution is proposed, based on the results of the temperature

measurements in various selected points within the tissue ablation zone and on the consideration of the computed cell death area. The solution involves the following procedure:

Step 1: Acquisition of the experimental data of electrical conductivity for each selected tissue at the frequency of interest and different constant heating rates, from slow ($\sim 3\,°C/min$ or lower) to fast ($\sim 10\,°C/min$ or higher) heating rates, and normalization of the results to the reference conductivity (σ_{37m}) of the measured tissue. Note that this step can be omitted if the experimental data mentioned here is available.

Step 2: A preliminary simulation of the RFTA situation is performed, modeling the temperature dependence of electrical conductivity using a linear function such as equation (5). In this context a representative point is selected within the ablation zone of the considered tissue and here the time average of the heating rate is computed (HR_{TAV}).

Step 3: The time average of the heating rate obtained in the step 2 is compared with the constant heating rates of the experimental data mentioned in the step 1. As a result, the normalized data of the electrical conductivity with the constant heating rate closer to the time-averaged heating rate is selected.

Step 4: The selected data in the step 3 is multiplied by the reference conductivity (σ_{37s}) of the tissue to be simulated and the result is used in the final RFTA simulation. Note that for the same tissue type, because the characteristics of the β dispersion and the static conductivity are sensitive to the viability and time after death when the measurements were made, the reference conductivity of the measured tissue and the reference conductivity of the tissue to be simulated are not always necessarily same.

The point mentioned in the step 2 is the point equidistant from the ends of the portion of the active electrode inserted in the tissue, at which the temperature of the tissue reaches its maximum value at the end of the ablation process. The above procedure was applied to the experimental data of the normal liver tissue obtained by Deás et al [15] at three heating rates (0.1, 3 and 10 °C/min) and two RF frequencies (20 and 450 kHz). As a result, for both frequencies the data with the slow heating rate of 3 °C/min was selected. In the selected point, the time average of the heating rate for the frequency of 20 kHz was 3.33 °C/min when modeling the temperature dependence of electrical conductivity based on the equation (5), and 2.98 °C/min when modeling that dependence based on the interpolating curve of the selected slow heating rate of Deás et al [15]. For the frequency of 450 kHz the obtained values were 4.57 °C/min and 4.05 °C/min, correspondingly.
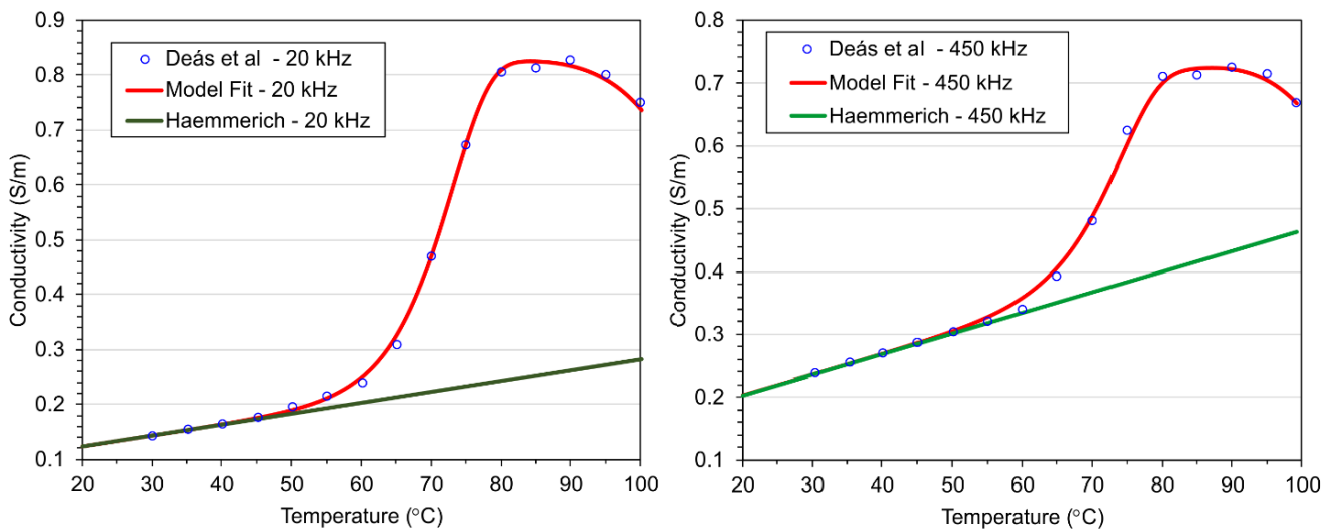

Figure 3

A comparison between three different models of the temperature dependence of electrical conductivity for the normal liver tissue (the selected slow heating rate data of Deás et al [15], an Arrhenius based conductivity model fit using the equation (13), and a model of the temperature dependence of electrical conductivity based on the linear equation (5) used by Haemmerich & Schutt [16]) for the frequencies of 20 and 450 kHz.

In Figure 3 a comparative plot of the selected data for both considered frequencies, an Arrhenius based conductivity model of these (model fit) using the equation (13), and the model of the temperature dependence of electrical conductivity based on the linear equation (5) used by Haemmerich & Schutt [16] is shown. A substantial agreement between the model fit and

experiments can be noted. The experimental results of Deás et al [15] suggested that the initial rise in conductivity (the linear part of the $\sigma(T)$ curve) is due to temperature only and is not time dependent, whereas the subsequent increase in conductivity during heating is due to irreversible structural changes that occur in tissue as a function of time during heating. In other words, conductivity of liver tissue exhibits a time–temperature dependence that can be modeled as two separate processes: a reversible temperature-dependent effect, and a permanent effect due to structural changes that occur during heating. There is a physical reason for the observed behavior. The changes in the conductivity in the nonlinear part of the $\sigma(T)$ curve are connected to the rupture of cellular and intracellular membranes that lead to leakage of cellular contents (water, ions and micro- and macromolecules) into the extracellular space, and to the phase change of tissue water that occurs at higher temperatures (vapor bubbles are formed close to the active electrode as a result of liquid evaporation and boiling). It is important to highlight that temperature threshold near 50 ℃ does not correspond to the notion of thermal damage due to protein denaturation, which takes place at much lower temperatures.

Figure 4 shows the temperature profile at the end of the 12-min ablation period determined from the computational models at 20 and 450 kHz using the interpolating curves of the selected slow heating rate data of Deás et al [15]. As in [16], significantly higher temperatures are observed in the tumor gel phantom when electric current is applied at 20 kHz, compared to normal tissue. This preferential heating of the tumor phantom is due to the frequency dependence of electrical tissue conductivity, and the much higher conductivity differential between normal and tumor tissues at 20 kHz compared to 450 kHz. Figure 5 shows the cell-survival fraction after 2 min and after 12-min heating at both frequencies, as calculated from the temperature profile history data of the computational model.
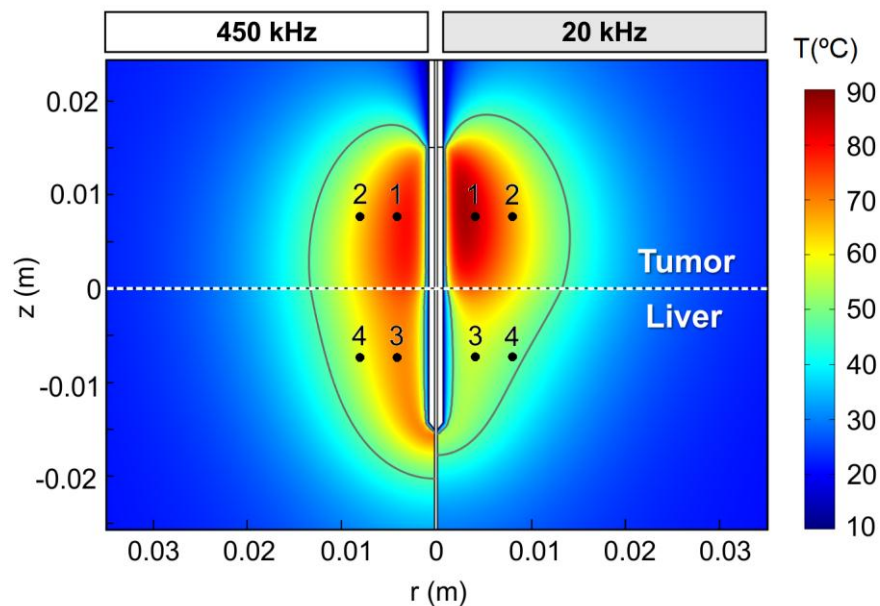

Figure 4

Temperature profile at the end of the 12-min ablation period determined from the computational models at 20 and 450 kHz using the interpolating curves of the selected slow heating rate data of Deás et al [15]. The dark gray boundary marks the region within which the estimated cell survival in the computer simulation is less than 1%. The marked locations are the points (1, 2, 3, and 4) where the temperature was measured in the corresponding experimental setup in [16].

Table I shows the temperatures measured and simulated by Haemmerich & Schutt [16] and those simulated here in the marked points of Figure 3 at 20 kHz and 450 kHz. It can be noted that, except for the points 3 and 4 of the normal tissue at 20 kHz, all the values of the simulated temperatures in our work are closer to the measured ones than the values simulated by Haemmerich & Schutt in their work. This result could be a consequence of the use of a more realistic model of the temperature dependence of electrical conductivity for the normal tissue. However, as it will be seen below, the major impact of this model is on the results of the quantification of the cell death area.

While there is a better correlation between the experimental and the computational modeling data than in Haemmerich & Schutt [16] work, there is still a notable difference in terms of absolute temperature values. The reason for this deviation, as suggested by Haemmerich & Schutt [16], could be the fact that the axisymmetric 2D geometry used in the simulations not

Douglas Deás Yero, Fidel Gilart González, Dirk Van Troyen, Guy A.E. Vandenbosh

reproduce the exact 3D geometry of the experimental setup (i.e., size and form of various layers, saline, location of ground electrode, etc.), e.g., a considerable fraction of applied power may be dissipated in the saline resulting in reduced energy deposition and heating of the tissue and gel layers compared to the computer simulation. In addition, melting of the gel phantom and resulting convection, as well as the assumed electrical and thermal properties for the gel phantom may affect results. Due to higher temperatures in the tumor phantom at 20 kHz than at 450 kHz, the melting of this medium as well as its assumed electrical and thermal properties could be the possible cause for the observed deviation of the simulated temperatures in comparison with the measured ones in the case of the points 3 and 4 at the frequency of 20 kHz.
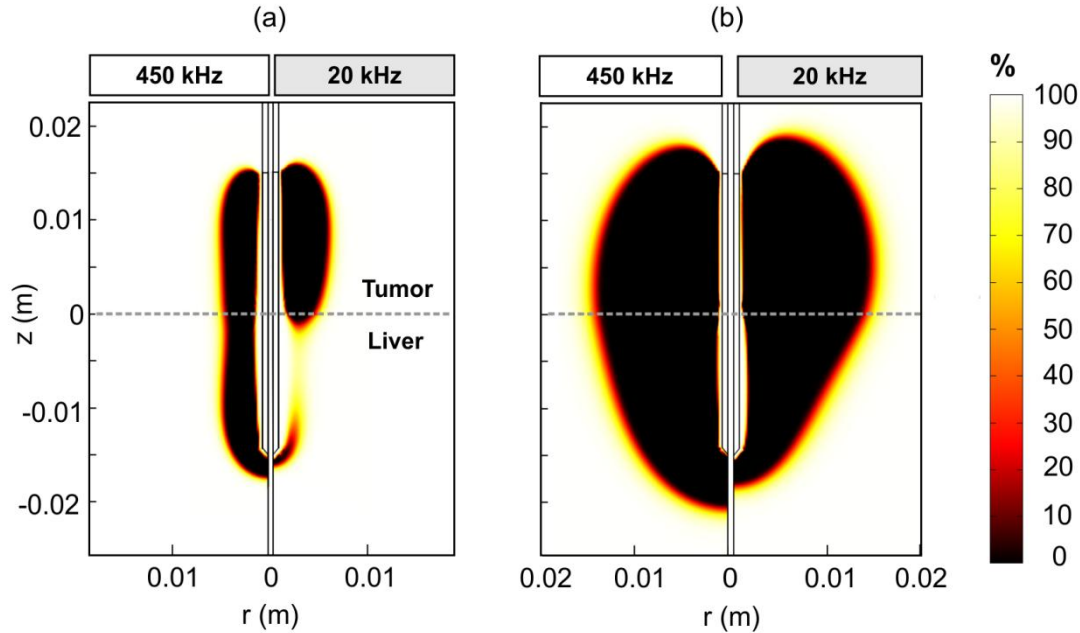

Figure 5

Cell-survival fraction (%) after 2 min (a) and after 12-min (b) heating at both frequencies, as calculated from temperature history using the interpolating curves of the selected slow heating rate data of Deás et al [15].

Table I

Temperatures measured and simulated in the marked points of Figure 3 at 20 and 450 kHz.

Frequency	Result	Temperature °C			
		Tumor phantom		Liver Tissue	
		Point 1	Point 2	Point 3	Point 4
20 kHz	Experimental - Haemmerich	76.9±5.6	65.6±2.0	64.6±7.7	57.2±5.6
	Simulation - Haemmerich	99.9	83.7	67.2	58.4
	Simulation - This work	84.87	67.87	55.80	49.20
450 kHz	Experimental - Haemmerich	65.1±1.3	57.5±1.4	65.8±3.0	58.7±2.5
	Simulation - Haemmerich	83.7	69.2	83.8	69.2
	Simulation - This work	77.69	62.99	68.74	57.29

Table II

Material properties used by Haemmerich & Schutt [16] in their computer models.

Material	$\sigma(\mathbf{S/m})$	$\rho(\mathbf{kg/m^3})$	$c(\mathbf{J/(kg \cdot K)})$	$k(\mathbf{W/(m \cdot K)})$
Liver tissue	$\sigma = \sigma_0[1 + 0.0162(T - 20)]$ $\sigma_0(450\text{ kHz}, 20\text{ °C}) = 0.2028$ $\sigma_0(20\text{ kHz}, 20\text{ °C}) = 0.1225$	1060	$c = \begin{cases} c_0 & T \leq 63.5\text{ °C} \\ c_0 + k_c(T - 63.5) & T > 63.5\text{ °C} \end{cases}$ $c_0 = 3800$ $k_c = 28.9\text{ J/(kg} \cdot \text{K}^2)$	$k = 0.498 + 0.0008. T(\text{°C})$
Tumor phantom	0.2439 (20 °C)	998 (20°C)	4182 (20°C)	0.6 (20°C)

Table II shows the tissue and tumor phantom material properties used by Haemmerich & Schutt [16] in their computer models. For the tumor phantom, they assumed that thermal properties and their temperature dependence were the same as for water. For electrical conductivity of both liver tissue and gel phantom, they used the average of the values they

Douglas Deás Yero, Fidel Gilart González, Dirk Van Troyen, Guy A.E. Vandenbosh

measured in the experimental part of their study, both at 20 and 450 kHz. For the agar phantom, they assumed electrical conductivity to vary with temperature as it does for a 0.12 % NaCl solution. As a muscle phantom they used a 0.25 % NaCl solution because its conductivity is practically similar as muscle tissue at both considered frequencies.
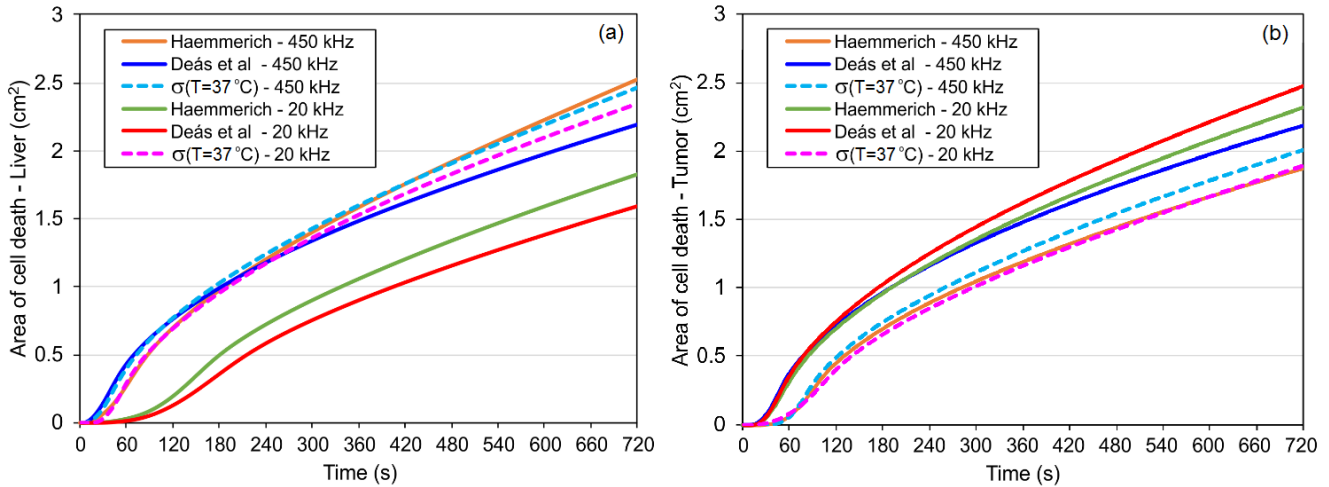

Figure 6

Computed cell death area in the normal tissue (a) and tumor phantom (b) during the ablation process, using three different models of the temperature dependence of electrical conductivity (interpolating curve of the selected slow heating rate data of Deás et al [15], linear equation from Haemmerich & Schutt [16], and constant $\sigma=\sigma_{37}$) at 450 kHz and 20 kHz.

Figure 6 compares the effects of three different models of the temperature dependence of electrical conductivity (interpolating curve of the selected slow heating rate data of Deás et al [15], linear equation from Haemmerich & Schutt [16], and constant $\sigma = \sigma_{37}$) on the computed cell death area (the lesion size) in the normal tissue and tumor phantom during the ablation process at 20 kHz and 450 kHz. It can be noted that, contrary to the results obtained in the simplified RFTA situation studied in [7] at 480 kHz where the authors concluded that all tested models were suitable for the simulation of RFTA as long as the conductivity variation with temperature is taken into account, in the more complex RFTA situation considered here, in general all tested models had a different impact on the computed cell death area. From Figure 6 it is evident that at 450 kHz the effects of the linear model of Haemmerich & Schutt [16], and of the constant $\sigma = \sigma_{37}$ model on the computed cell death area are practically similar in the normal tissue and tumor phantom, however they are remarkably different at 20 kHz. It can be noted also that for the Haemmerich & Schutt model the computed cell death area at 450 kHz is always greater in the normal tissue than in the tumor phantom, however at 20 kHz an opposite behavior is observed. Regarding the constant $\sigma = \sigma_{37}$ model, at both frequencies the computed cell death area is always greater in the normal tissue than in the tumor phantom. Finally, in the case of the model based on the interpolating curve of the selected slow heating rate data of Deás et al [15], the computed cell death area at 450 kHz is always practically equal in the normal tissue and in the tumor phantom, whereas at 20 kHz it is always lesser in the normal tissue than in the tumor phantom. Moreover, in this case the cell death area differential is remarkably greater than the corresponding differential in the case of the Haemmerich & Schutt model at the same frequency.

During RF ablation the tissue heating, and thus the extent of the thermal lesion, is largely influenced by tissue-dependent parameters, such as electrical conductivity and perfusion other than by device-dependent factors (e.g. type of applicator, applied power). Ideally, such tissue-dependent parameters and their changes during heating should be known to enable individual planning of the medical procedure. Knowledge of these properties would enable the development of accurate simulation-based frameworks for individual planning of RFTA [36]. From a practical point of view, the patient-specific value of such parameters can be known only at body temperature while the changes during heating must be investigated in animal studies in in vivo or ex vivo experiments. The aims of this study were two: (1)- to propose a reasonable procedure for selecting the appropriate experimental data for the simulation, taking into account the heating rate at which the data was acquired and the power that will be delivered to the electrodes in the RFTA, and (2)- to determine whether the models of the temperature dependence of electrical conductivity used in the simulations in a complex RFTA situation, entailing the presence of multiple materials with different dielectric properties, affects the computed extent of the thermal lesion.

Although it is known that the electrical conductivity strongly affects the power distribution within the tissue and thus the extent of the thermal lesion, the fundamental parameter to validate any practical RFTA model, the identification of the large impact that the models of the temperature dependence of electrical conductivity have on the lesion size prediction in a

typical RFTA situation, as the one considered here, has not been made before. In contrast to [17], our results demonstrate that not only the initial (baseline) electrical conductivity is important in predicting the lesion size, but also it is the model of the temperature dependence of electrical conductivity.

It should be noted that in the Haemmerich & Schutt [16] and our numerical simulations the model of a tumor gel phantom was used instead of the model of a tumor tissue. On the other hand, in neither of these works a measurement of the thermal lesion was carried out. Therefore, the conductivity models must also be tested in a more realistic RFTA situation involving the model of a tumor tissue instead of the model of a tumor gel phantom, and the predicted lesion size should be confirmed experimentally.

While we could not confirm experimentally the results shown in Figure 6 as the gel phantom does not allow visualization of the coagulation zone, we have used a more realistic model for the conductivity of the liver tissue than those used before and have obtained a better agreement with the temperature data in comparison with Haemmerich & Schutt [16]; reason why one can expect that when simulating RFTA the better results for the predicted cell death area must be obtained when using our conductivity model.

4. CONCLUSIONS AND FUTURE WORKS

A reasonable procedure was proposed for selecting the appropriate experimental data of the temperature dependence of electrical conductivity for the simulation, taking into account the heating rate at which the data was acquired and the power that will be delivered to the electrodes in the RFTA situation of interest, based on the computing of the time average of the heating rate in a representative point of the ablation zone. The numerical results confirmed that the use of lower frequencies (20 kHz) than currently used during RFTA (450 kHz) may result in preferential heating of the tumor and consequently in less damage on healthy tissue. This paradigm may have implications for targeted tumor destruction and device design. Also, the effect on the computed thermal lesion size of three different models of the temperature dependence of electrical conductivity used for the simulation of a RFTA situation at 20 and 450 kHz, entailing the presence of three materials with different dielectric properties (normal liver tissue, tumor gel phantom and muscle saline phantom) was investigated. The results demonstrated that not only the initial (baseline) electrical conductivity is important in predicting the lesion size, but also it is the model of the temperature dependence of electrical conductivity. However, the conductivity models must also be tested in a more realistic RFTA situation involving the model of a tumor tissue instead of the model of a tumor gel phantom, and the predicted lesion size should be confirmed experimentally. Future studies should address these topics.

ACKNOWLEDGMENTS

REFERENCES

1. Trujillo M, Berjano E. Review of the mathematical functions used to model the temperature dependence of electrical and thermal conductivities of biological tissue in radiofrequency ablation. International Journal of Hyperthermia. 2013;29(6):590–7.

2. Haemmerich D, Chachati L, Wright AS, Mahvi DM, Lee FT, Webster JG, et al. Hepatic Radiofrequency Ablation With Internally Cooled Probes: Effect of Coolant Temperature on Lesion Size. IEEE Transactions on Biomedical Engineering. 2003;50(4):493–500.

3. Pop M, Molckovsky A, Chin L, Kolios MC, Jewett MAS, Sherar MD. Changes in dielectric properties at 460 kHz of kidney and fat during heating: importance for radio-frequency thermal therapy. Physics in Medicine and Biology. 2003;48(4803):2509–25.

4. Lobo SM, Liu ZJ, Yu NC, Humphries S, Ahmed M, Cosman ER, et al. RF tumour ablation: computer simulation and mathematical modelling of the effects of electrical and thermal conductivity International Journal of Hyperthermia. 2005; 21:199–213

5. Liu Z, Lobo SM, Humphries S, Horkan C, Solazzo SA, Hines-Peralta AU, et al. Radiofrequency tumor ablation: insight into improved efficacy using computer modeling. American Journal of Roentgenology. 2005;184:1347–52

6. Ahmed M, Liu Z, Humphries S, Goldberg SN. Computer modeling of the combined effects of perfusion, electrical conductivity, and thermal conductivity on tissue heating patterns in radiofrequency tumor ablation. International Journal of Hyperthermia. 2008;24:577–88

7. Macchi EG, Gallati M, Braschi G, Persi E. Dielectric properties of RF heated ex vivo porcine liver tissue at 480 kHz: measurements and simulations. Journal of Physics D: Applied Physics. 2014;47(48):485401.

8. Schwan HP. Electrical properties of tissues and cell suspensions Advances in Physics in Medicine and Biology. 1957;5:147–209.

9. Gabriel C, Gabriel S, Corthout E. The dielectric properties of biological tissues: part I. Literature survey Physics in Medicine and Biology; 1996;41:2231–49

10. Gabriel S, Lau RW, Gabriel C. The dielectric properties of biological tissues: part II. Measurements in the frequency range 10 Hz–20 GHz. Physics in Medicine and Biology. 1996;41:2251–69.

11. Gabriel S, Lau RW, Gabriel C. The dielectric properties of biological tissues: part III. Parametric models for the dielectric spectrum of tissues. Physics in Medicine and Biology. 1996;41:2271-2293.

12. Camelia Gabriel. Dielectric Properties of Biological Materials. In: Frank S. Barnes, Ben Greenebaum, editors. Bioengineering and Biophysical Aspects of Electromagnetic Fields. U.S.A.: CRC Press Taylor & Francis Group; 2007.

13. Ryan T, Platt R, Dadd J, Humphries S. Tissue electrical properties as a function of thermal dose for use in a finite element model. Advances in Heat and Mass Transfer in Biotechnology. 1997;24(355):167–71.

14. Zurbuchen U, Holmer C, Lehmann KS, Stein T, Roggan A, Seifarth C, et al. Determination of the temperature-dependent electric conductivity of liver tissue ex vivo and in vivo: Importance for therapy planning for the radiofrequency ablation of liver tumours. International journal of hyperthermia. 2010;26(1):26–33.

15. Deás Yero D, González FG, Troyen D Van, Vandenbosch GAE. Dielectric properties of ex - vivo porcine liver tissue characterized at frequencies between 5 and 500 kHz when heated at different rates. IEEE Transactions on Biomedical Engineering. 2018; 65(11) 2560-2568.

16. Haemmerich D, Schutt DJ. RF ablation at low frequencies for targeted tumor heating: In vitro and computational modeling results. IEEE Transactions on Biomedical Engineering. 2011 Feb;58(2):404–10.

17. Hall SK, Ooi EH, Payne SJ. Cell death, perfusion and electrical parameters are critical in models of hepatic radiofrequency ablation. International Journal of Hyperthermia. 2015;31:538–50.

18. Chiang J, Wang P, Brace C. Computational Modelling of Microwave Tumour Ablations. International Journal of Hyperthermia. 2013;29(4):308–17.

19. Berjano EJ. Theoretical modeling for radiofrequency ablation: state-of-the-art and challenges for the future. Biomedical engineering online. 2006;5(1):24.

20. Panescu D, Whayne JG, Fleischman SD, Mirotznik MS, Swanson DK, Webster JG. Three-Dimensional Finite Element Analysis of Current Density and Temperature Distributions. IEEE Transactions on Biomedical Engineering. 1995;42(9).

21. Shao YL, Leo HL, Chua KJ. Studying the thermal performance of a bipolar radiofrequency ablation with an improved electrode matrix system: In vitro experiments and modelling. Applied Thermal Engineering. 2017;116:623–35.

22. Jamil M, Ng EYK. Quantification of the effect of electrical and thermal parameters on radiofrequency ablation for concentric tumour model of different sizes. Journal of Thermal Biology. 2015;51:23–32.

23. Dodde RE, Miller SF, Geiger JD, Shih AJ. Thermal-Electric Finite Element Analysis and Experimental Validation of Bipolar Electrosurgical Cautery. Journal of Manufacturing Science and Engineering. 2008;130(2):1087–357.

24. Wang Z, Aarya I, Gueorguieva M, Liu D, Luo H, Manfredi L, et al. Image-based 3D modeling and validation of radiofrequency interstitial tumor ablation using a tissue-mimicking breast phantom. International Journal of Computer Assisted Radiology and Surgery. 2012;7(6):941–8.

25. Haemmerich D, Tungjitkusolmun S, Staelin ST, Lee FT, Mahvi DM, Webster JG. Finite-element analysis of hepatic multiple probe radio-frequency ablation. IEEE Transactions on Biomedical Engineering. 2002;49(7):836–42.

26. Fang Z, Zhang B, Moser M, Zhang E. Design of a Novel Electrode of Radiofrequency Ablation for Large Tumors : A Finite Element Study. Journal of Engineering and Science in Medical Diagnostics and Therapy. 2018;1(February):1–6.

27. Wang Z, Member S, Luo H, Coleman S, Cuschieri A. Bi-component conformal electrode for radiofrequency sequential ablation and circumferential separation of large tumours in solid organs : development and in-vitro evaluation. IEEE Transactions on Biomedical Engineering. 2016;9(2):1–7.

28. Schutt DJ, Haemmerich D, Schutt DJ. Effects of variation in perfusion rates and of perfusion models in computational models of radio frequency tumor ablation Effects of variation in perfusion rates and of perfusion models in computational models of radio frequency tumor ablation. Medical Physics. 2008;35(8):3462–70.

29. Stogryn A. Equations for Calculating the Dielectric Constant of Saline Water (Correspondence). IEEE Transaction on Microwave Theory and Techniques. 1971;1(19):733–6.

30. Haemmerich D, Schutt DJ, Webster JG, Mahvi DM. In vitro measurements of temperature-dependent specific heat of liver tissue. Medical Engineering & Physics. 2006;28:194–7.

31. I Dos Santos, D Haemmerich, D Schutt, AF da Rocha LRM. Probabilistic finite element analysis of radiofrequency liver ablation using the unscented transform. Physics in Medicine and Biology. 2009;54(3):627.

32. S Arrhenius, On the rate of the inversion of cane sugar by acids. Zeitschrift für Physikalische Chemie. 1889;4:226–248.

33. KR Diller, JA Pearce. Issues in modeling thermal alterations in tissues. Annals of NY Academy of Sciences. 1999; 888(1):153–164.

34. Goutham R, Matthew RD, Christian R, Bradford JW, D Haemmerich. Cytotoxicity of hepatocellular carcinoma cells to hyperthermic and ablative temperature exposures: In vitro studies and mathematical modelling. International Journal of Hyperthermia. 2013;29(4):318–323.

35. MS Breen, M Breen, K Butts, L Chen, GM Saidel, DL Wilson. MRI-guided thermal ablation therapy: Model and parameter estimates to predict cell death from MR thermometry images. Annals of Biomedical Engineering. 2007;5(8):1391–1403.

36. Zhang B, Moser MAJ, Zhang EM, Luo Y, Liu C, Zhang W. A review of radiofrequency ablation: Large target tissue necrosis and mathematical modelling. Physica Medica. 2016;7(92):1–11.

AUTHORS

Douglas Deás Yero, Electrical Engineer, MSc in Electrical Engineering from the Universidade Federal de Santa Catarina, Brasil, Centro Nacional de Electromagnetismo Aplicado, Santiago de Cuba, Cuba, Now he is working toward his PhD degree in Bioengineering from the Universidad de Oriente. His main research interests are in medical application of RF and microwave technique, particularly ablation and hyperthermia.
E-mail: douglas@uo.edu.cu.

Fidel Gilart González, BS in Physics, PhD in Physical Sciences from the Universidad de Oriente, Cuba, Centro Nacional de Electromagnetismo Aplicado, Santiago de Cuba, Cuba, His research interests are the interaction between nonionizing electromagnetic radiation and biological systems, and industrial and medical applications of electromagnetic fields, including design, modeling and simulations.
E-mail: fgg@uo.edu.cu.

Dirk Van Troyen, received the MSc degree in Industrial Engineering from KU Leuven Technology Campus Ostend in 1981, the MSc degree in Electronics Engineering from KU Leuven in 1987, the MSc in Mechanical-Electrotechnical Engineering from DHO-Brussels in 1999 and the PhD in Applied Sciences in 1995 from KU Leuven. His main research activities are EMC, Antennas and Propagation and R.F.-Radio Science. He is currently a Professor at the KU Leuven – De Nayer and C.E.O. of Laboratoria De Nayer.
E-mail: dirk.van.troyen@labodenayer.be

Guy A. E. Vandenbosch, received the MSc and PhD degrees in Electrical Engineering from the Katholieke Universiteit Leuven, Leuven, Belgium, in 1985 and 1991, respectively. From 1991 to 1993, he held a postdoctoral research position at the Katholieke Universiteit Leuven. His research interests are in the area of electromagnetic theory, computational electromagnetics, planar antennas and circuits, nano-electromagnetics, EM radiation, EMC, and bio-electromagnetics.
E-mail: guy.vandenbosch@esat.kuleuven.be